The 2014 World Congress on
Advances in Civil, Environmental, and Materials Research (ACEM14)
Busan, Korea, August 24-28, 2014

Characterization and evaluation of biochars derived from agricultural waste biomass from Gansu, China

*Baowei Zhao[1] and Obemah David Nartey[2]

[1), 2)]*School of Environmental and Municipal Engineering, Lanzhou Jiaotong University, Lanzhou 730070, P. R. China*

[1)]*baoweizhao@mail.lzjtu.cn*

ABSTRACT

Five biochars derived from cotton (*Gossypium herbaceum*) straw, cotton residue, potato (*Solanum tuberosum*) straw, potato residue and swine (*Sus scrofa domesticus*) manure, termed as BCCS, BCCR, BCPS, BCPR and BCSM, were characterized and evaluated. SEM micrographs showed that BCs had recognizable pore size which also contributed to their higher surface areas except BCSM450. XRD patterns showed peaks found at 2θ at d=3.35 Å and d=3.16-3.00 Å were related to quartz (SiO_2) and calcite ($CaCO_3$), respectively, while these peaks were non-recognizable in BCCS as a result of their amorphous nature. Proximate analysis showed that the highest moisture content in BCCR (9.65%) whereas BCSM recorded the highest ash content (15.22%). The elemental analysis showed that carbon content increased from 58.97 to 81.28%. Atomic ratios, polarity index and aromatic ratios also showed remarkable results. Surface areas for BCCR, BCCS, BCPR, BCPS and BCSM were 126.08, 443.96, 15.43, 30.84, and 67.88 m^2/g, respectively. The cationic exchange capacities (CEC) (48.26, 77.30, 34, 59.48 and 71.83 $cmol_c$/kg for BCCR, BCCS, BCPR, BCPS and BCSM), were determined, respectively. Boehm titration indicated that BCCS (8.85 mmol/g) and BCPR (2.25 mmole/g) showed the highest and lowest acidities. FTIR spectrum appears to be quite different for BCs. Common bands around 3600 and 1078 cm^{-1} were assigned to polymeric hydroxyl (R-OH) and carbonyl esters (C=O), respectively. The results demonstrated the potential of BC as an amendment to adsorb and immobilize heavy metals in loess soil.

1. INTRODUCTION

Biochar (BC), such as wood charcoal and crop residues-derived products, refers to the carbon rich residues from pyrolysis or incomplete combustion of biomasses. Bc has

[1)] Professor
[2)] Graduate Student

the ability to improve soil fertility, keep nutrient, mitigae climate change, and sequestrate carbon and helps in managing wastes (Marris, 2006; Lemann, 2007; Renner, 2007; Fraser, 2010; Keiluweit et al., 2010; Roberts et al., 2010; Zimmerman, 2010), which has been paid much attention.

BC has porous structure, negative charged surface and a large amount of functional groups (such as carboxyl, hydroxyl, phenoxyl and carbonyl, etc). These properties make BC be a remarkable adsorbent for contaminants when it is intentionally added into soils. The adsorption and immobilization of heavy metals by BC decrease the migration and availability of heavy metals and would be a promising in-situ alternative to remedy soils contaminated with heavy metals. Review of recent papers indicates that the electrostatic interaction attraction between BC and cations exist (Chen et al. 2011; Regmi et al., 2012). Inner-sphere surface complex formation is the strength interaction mechanism that involves both ionic and covalent bonds (Liang et al., 2010). For heavy metal, affinity to BC strength depends up on the configuration of the d-orbital electrons of cations and the functional groups of BC (Cao et al., 2009; Liu et al., 2009; Mohammed et al., 2011; Regmi et al., 2012). In some cases, precipitation is the main interaction between BC and heavy metals (Tong et al., 2011). Most BCs are not fully carbonised, including the carbonised (COM) and the non-carbonised organic matter (NOM). COM is suspected to behave as an adsorbent and NOM as a partition phase. The sorptions of BCs are controlled by the relative carbonised and non-carbonised fractions and their surfaces and the bulk properties are characteristics to consider (Chen et al., 2008). As mentioned above, the chemical structure and properties of BC play the key role in adsorption, immobilization and bioavailability of heavy metals.

All over the world, loess soil is widely spread, whose area is one-tenth of the earth land. About 640 thousand km^2 of loess topographically spread in China. On the one hand, loose structure, large porosity and water permeability, low agglomerating force and organic carbon content result in the loess soils nutrient leaching and being poorer. On the other hand, serious heavy metal pollution of the soils in this area has been found, which is mainly derived from water used for irrigation from industrial waster water, fertilizers and agrochemicals as well as sewage (Nan et al., 2000), due to less precipitation in loess area. Therefore, for the loess soil, it should be applied with BC, in order to improve soil structure and properties, increase soil water holding capacity, improve soil fertility and enhance crop yield. Meanwhile, it is also expected using BC as an admenture to control migration, transformation and bioavailability behaviour of heavy metal pollutants, and to ensure the safety of agricultural products.

To our knowledge, there were few studies concerned the BCs from the agricultural waste in loess area. This paper aims to evaluate the chemical and physical properties of BCs produced from various sources of agricultural wastes, namely cotton residue, cotton straw, potato residue, potato straw and swine manure. They are aboundantly in Gansu Province, China, where loess soil is widely spread and the envionemntal problems caused by heavy metal are serious. The results could be merited for application of BCs from loess area.

2 MATERIALS AND METHODS

2.1 Biomass

Cotton (*Gossypium herbaceum*) straw and residue samples were collected from local farmland and Cotton Processing Co. Ltd. in Dunhuang, China. Potato (*Solanum tuberosum*) straw and residues were sampled from local farmland and Potato Starch Co. Ltd. in Dingxi, China. Swine (*Sus scrofa domesticus*) manure was supplied from local piggery in Anning District, Lanzhou, China. The biomasses were air dried for 7 days at an average temperature of 18 ^{o}C. After a weeklong drying, all samples were initially washed with tap water three consecutive times and finally washed with deionised water. After oven dried for 48 hr at 80 ^{o}C, the samples were partially grounded using a pulveriser into smaller sizes.

2.2 Pyrolysis procedure

Pyrolysis of each biomass took place in a ceramic pot with a pressed state that was 8.5 cm long and diameter of 9.0 cm. After the ceramic pot was filled with the 30 g of the dried biomass, it was placed in an electric furnace (Shanghai Laboratory Equipment Company Limited, KSW 12-11) for the start at the charring process at limited oxygen condition. The furnace was heated by a step wise manner at a residence time of 3 hr. The initial starting temperature was set at 100 ^{o}C, and subsequently elevated to 250 ^{o}C (each temperature was maintained for 3 hr), and then to the target temperature. After 3 hr of heating and charring, the hot ceramic pots were carefully removed out and cool overnight. Each biomass was produced at 250, 300, 350, 400, 450, 500, 550, 600, 650 and 700 ^{o}C to obtained fifty (50) samples for further purposes.

2.3 Post-biochar treatment

20 g of each carbonized sample is added to 100 mL 1.0 M HCl in a 250 mL beaker. The beaker and its content in a covered state were placed in a reciprocating shaker (Jiangsu Laboratory Equipment Company Limited, THZ-82A, China) and agitated at 180 rpm for 30 min at 25 ^{o}C. The resultant is allowed to settle for 12 hr and finally separated by vacuum filtration. The residues were rinsed with deionised water until the aqueous phase becomes neutral. The BCs were oven dried for 24 hr at 105 ^{o}C and finally sieved through 0.4-0.25 mm mesh. These BCs are hereafter referred to as BCCR250-BCCR700, BCCS250-BCCS700, BCPR250-BCPR700, BCPS250-BCPS700 and BCSM250-BCSM700, for cotton residue, cotton straw, potato residue, potato straw and swine manure, respectively, where the suffix number represents the pyrolytic temperature. Batch adsorption experiments, each run with 0.5 g of BC in 20 mL of 10 mg/L Pb(II) solution (pH = 5.3) at 25 ^{o}C for 24 h, were carried out and the maximum adsorptive capacities were found with BCCR600, BCCS650, BCPS500, BCPR650 and BCSM450. Then the corresponding BC was used to be characterized.

2.4 Characterization of BC

Scanning electron microscopy (SEM) of the samples were taken using Hitachi S-4800SEM, H1-9021-004, Japan, which was operated at a vacuum mode under an accelerating voltage of 5 kV, calibration scan speed of 25, using secondary electrons. X-ray Diffraction spectra were obtained using a high resolution X-ray diffractometer

(PANalytical X'Pert Pro, CuKα, radiation source at 35 kV voltages, 25 mA current) and a miniflex goniometer was used for the XRD analysis at room temperature. Diffraction patterns were collected in the 2θ range of 3 – 90^o at a scan speed of 1^{o}min^{-1} and a step size of 0.02^o. Elemental analysis was completed by the Vario EL cube V1.2.1 Elementar Analyze, Germany. The total contents of C, N, H, and S were determined by the analyzer whiles the oxygen (O) content was determined by subtracting the ash, C, N, H, and S contents from the total mass of the sample. The surface areas and related determinations were determined by using multiple BET analysis on a Micrometric, ASAP 2010 (Surface area and porosity analyzer, USA) system. Boehm titration was conducted to determine surface acidity and alkalinity according the reference. Fourier transform infra-red resonance (spectroscopy) (FTIR) were analysed using a Nicolet 6700-FTIR (Nexus 6700-FTIR, USA) spectroscopy. Cation Exchange Capacity (CEC) of BCs were determined according to the method of CEC determination in alkaline solution (Carrier et al., 2012). Proximate analysis refers to the aspect of physical characterization which basically looks at moisture and ash content of BC. Moisture content determines the amount of water that can be available in the BC whiles the ash content looks at the amount of the BC that can be converted into ash at a specific temperature.

3. RESULTS AND DISCUSSIONS

3.1 Scanning electron microscopy (SEM)

SEM micrographs of BCPR, BCPS, BCCS, BCCR and BCSM samples were shown in Fig. 1. The five different BCs product at different pyrolytic temperature had a distinguishable honey comb like structure except BCSM due to the presence of tubular structures originally emanating from plant cells. Between BCPR, BCPS, BCCS and BCCR, there were recognizable differences. The SEM micrographs of BCCS and BCCR obtained from cotton straw and cotton residue were found to have many orderly pores over the surface, forming a system of developed pore structures. As a result of these well-developed pores, the BCs possessed a high BET surface area (452.9 m^2/g and 126.08 m^2/g for BCCS and BCCR, respectively).

BCPS, BCPR and BCSM have lower BET surface areas as a result of the shrinkage of BCs at post softening in narrowing or closing pores. These observations can be confirmed from the SEM micrographs. BCSM does not have a considerable porous structure, as again confirmed by its low BET surface area. SEM images of BCSM showed that the interior parts of these BCs are filled and are not porous. Similar results were also observed by Regmin et al. (2012), Angin (2013) and Gao et al.. (2013).

It can be concluded from the BET analysis (Table 2) and SEM micrographs of BC samples that BC have some internal pores whiles the pores of BCSM were not characteristically found. Therefore, it is positive to use BC samples especially from cotton straw, cotton residue and potato straw as a carbon feedstock for producing carbon

materials such as BC, activated carbon, carbon nonatubes and carbon fibre for immobilization of pollutants from the environment.

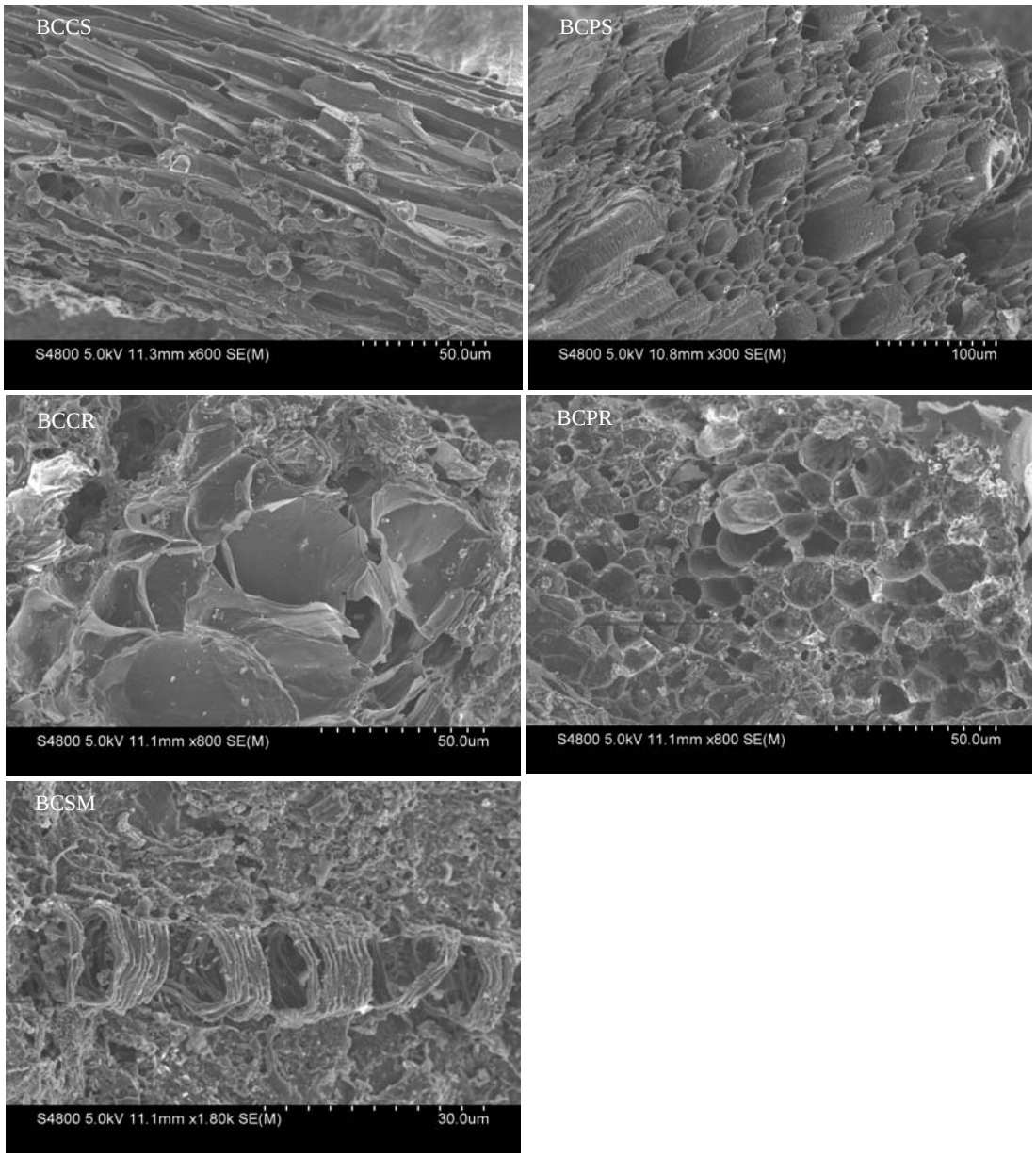

Fig. 1 Photomicrograph from SEM

3.2 X-Ray Diffraction

The XRD patterns for BC are shown in Fig. 2 In the most cases, three groups of diffraction patterns were normally observed over the examined 2θ range (3-90^{o}), which corresponds to the diffuse graphite peaks in low and high theta regions respectively. In general, diffuse and broad bands in XRD patterns characterize the existence of short range order in the carbon structure, while the sharp and narrow peaks confirms to highly crystalline phases with high degree of long-range order. In carbon solids with a long-term structural order, this is attributed to the loading of the graphitic basal planes, is usually observed at a 2θ value of 25^{o}.

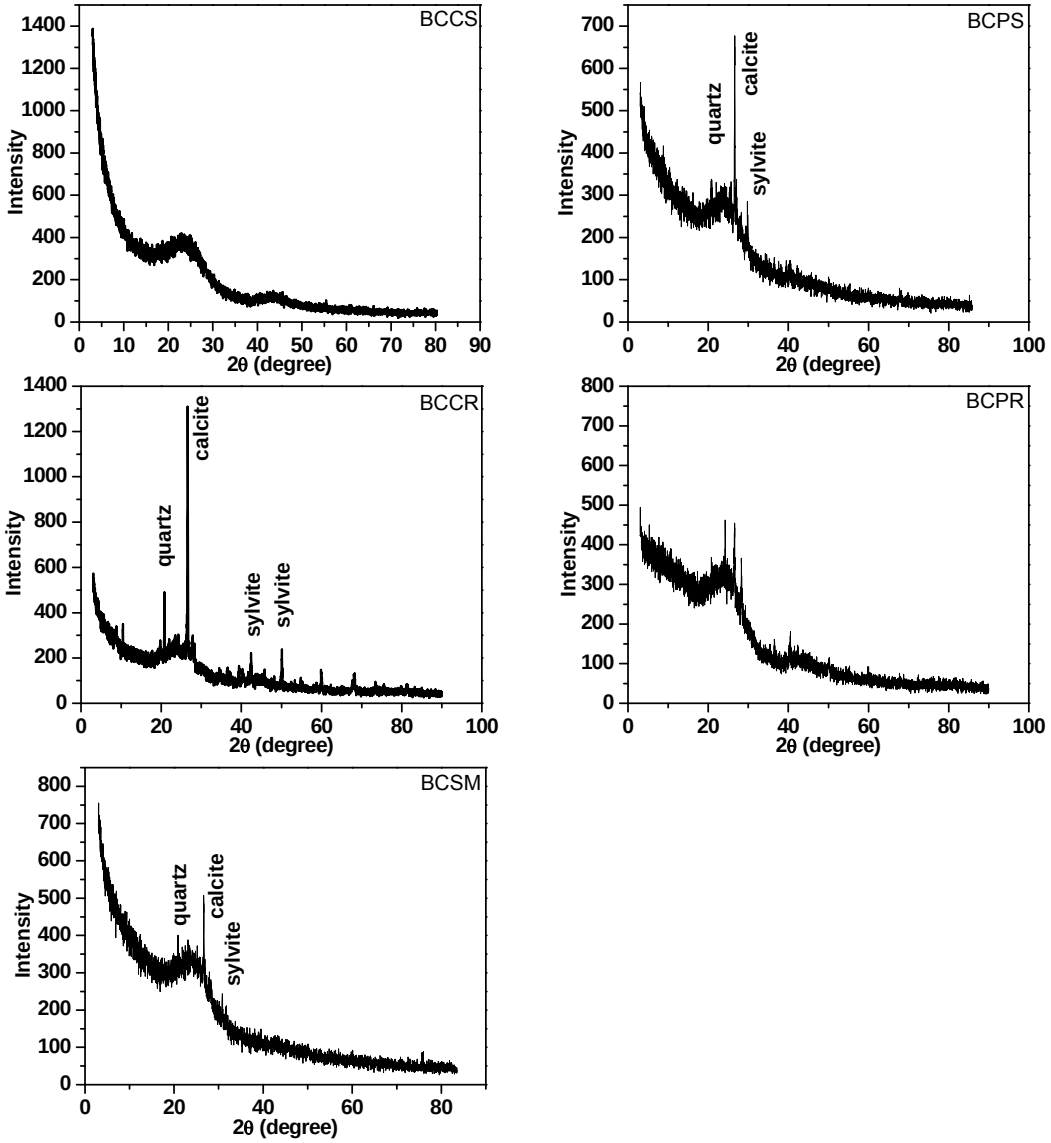

Fig.2 XRD patterns of BCs

Again as shown in Fig. 2 there are distinct sharp crystalline peaks found, at 2θ at 26.6^{o} (d=3.35 Å) and 29-29^{o} (d=3.16-3.00 Å) which probably indicated the presence of quartz (SiO_2) and calcite ($CaCO_3$) respectively, whereas these peaks were absent in BCCS. The absence of any crystalline peak of cellulose in the BCCS XRD pattern confirms that it contained mainly the amorphous compounds as a result of the decomposition of cellulose indicating an amorphous carbon structure with randomly oriented aromatic carbon sheets. In addition to calcite, quartz and graphite, some associated minerals crystals, such as sylvite (KCl), periclase (MgO) and whitelodcite ((Ca, $Mg)_3(PO_4)_2$) can also be found in the BC samples.

3.3 Proximate analysis

Amount of moisture in a BC is the mineralized water content in living cells, containing anions, cations and non-charged species. The determined ash contents (%) for BCCR, BCCS, BCPS, BCPR and BCSM were 4.58, 3.36, 7.78, 15.6 and 5.22 while the moisture contents were 9.65, 7.82, 6.64, 7.18 and 7.12, respectively. The moisture contents of cotton straw, potato residue and swine manure (7.1-7.8%) were similar to each other, whereas potato straw (6.64) had relatively lower moisture content and cotton residue (9.65%). The moisture content in raw biomass would affect the energy consumption and decrease the efficiency of the conversion process and also increase the cost of transport (Agirre et al., 2013).

As far as the ash content is concerned, swine manure (15.22) and potato residue (15.6%) recorded the highest ash content than potato straw (7.78%), cotton residue (4.58%) and cotton straw (3.36%). This could be related to environmental conditions (e.g. soil type, mode of industrial and agricultural waste generation, fertilizers used in farming, and other climatic conditions such as rainfall, sunshine, humidity, temperature, etc.). The ash content which were determined by proximate analysis, were higher for manure based biomass (swine manure) but lower for straw based biomasses (cotton straw). The ash content in the swine manure derived BC was also significantly higher than those carbon-like materials; this might probably be due to the presence of considerable amount of minerals such as calcite ($CaCO_3$) and quartz (SiO_2) in the manure feedstock. These results are consistent with the XRD (Fig. 2) results. The in homogeneity of the biomasses might also contribute to the ash content.

3.4 Elemental analysis

Table 1 shows the elemental analysis results. The H/C, O/C, C/N, (O+N)/C, (S+O)/C and (O+N+S)/C atomic ratios are important for BC characterization. O/C and H/C ratios indicate the degree of functionalization. These ratios were calculated to evaluate the aromaticity (H/C) and polarity (O/C). Functional groups consist basically of O or H, therefore O/C and H/C ratios show the presence of functional groups which increase adsorption of environmental pollutants (Zhang et al., 2013).

BCCR and BCPS showed the highest O/C ratio, while BCPS and BCSM showed the highest H/C ratio, while lowest O/C were observed for BCSM as well as lowest H/C were observed for BCCS. This trend showed that these BCs were less hydrophilic, which is due to less oxygen content. Therefore, more organic surface functionalities would be expected

on BCCR and BCPS than BCCS. These results were in consistent with the FTIR results obtained (Fig. 3).

C/N ratio of a BC is more related to the recalcitrant properties of the BC or it could be used to understand how much nitrogen could be mineralized. The C/N ratios of BCs wide-ranging between 16.16 and 82.38. BCCS showed the highest C/N ratio, which was similar to fast pyrolysis found in literature. It was observed that carbonization/pyrolysis leads to higher C content than the uncarbonized biomass. Therefore, lower C/N ratios of other BCs can be attributed to the nature of the biomass. Mostly, C/N ratios higher than 20 is expected to result in organic N immobilization by microbial biomass feedstock, which indices N differences for plants (Lehmann and Joseph, 2009). However, the aromatic nature of BC provides high recalcitrant against microbial decay. Consequently, it is unlikely that BCs would cause N immobilization.

The ratios of (O+N)/C as polarity index indicator increased in BCCR and again decreased in BCSM. These results show an increased aromaticity and decreased polarity of BCSM. The ratios of (O+N+S)/C, which and aromaticity factor, increased in BCCR and also decreased in BCSM. This trend seen in this analysis results may be attributed to the formation of aromatic structures by a higher degrees of carbonization of the organic matter and removal of polar surfaces functional groups, analogous to studies of Ahmed et al. (2012).

Table 1. Elemental composition and ash content of BCs.

BCs	C (%)	N (%)	H (%)	S (%)	Ash (%)	O (%)	(N+O) /C	(S+O) /N	H/C	O/C	C/N	(O+N+S)/ C
BCCR	58.97	2.5	1.7	0.27	4.45	32.1	0.59	12.95	0.029	0.544	23.59	0.591
BCPS	67.06	3.92	2.95	0.35	7.78	17.93	0.33	4.66	0.044	0.267	17.1	0.331
BCSM	70.32	4.19	3.18	0.41	15.22	6.68	0.15	1.7	0.045	0.095	16.79	0.16
BCCS	80.94	1.11	1.66	0.31	3.36	12.63	0.17	11.7	0.021	0.156	73.23	0.173
BCPR	65.72	3.42	2.05	0.22	15.12	13.47	0.26	4.01	0.031	0.205	19.24	0.26

Elemental composition and atomic ratios are on an ash-free basis. H/C: atomic ratio of hydrogen to carbon. O/C: atomic ratio of oxygen to carbon. (N+O)/C: atomic ratio of sum of nitrogen and oxygen to carbon. (S+O)/N: atomic ratio of sum of sulphur and oxygen to nitrogen. (O+N+S)/C: aromaticity. ND: not determined

3.5 Brunauer, Emmet and Teller (BET)

BET analyses of the BCs indicate the physical evaluation of BC pyrolysis which is generally connected with their sorption abilities. The surface area and porosity characteristics of the BC prepared in this present study are presented in Table 2.

BCCS (443.96 m^2/g) showed high surface areas, followed by BCCR (126.08 m^2/g), whereas BCPR (15.43 m^2/g) showed low surface area. The surface area of BC derived from pine coke, soya bean cake and peanut shells at 550 ^oC were found to be 208, 2.1, 11.8 and 211 m^2/g, respectively (Apaydin-Varol and Pütün, 2012). Similarly, study of Carrier et al. (2012) showed that between temperatures of 460-900 ^oC, the surface areas of BCs varied between 259-561 m^2/g for the vacuum pyrolysis of sugarcane bagasse. BCs from vacuum pyrolysis conditions such as pyrolytic temperature and heating rates,

pressure etc., and therefore greater devolatilization is often observed by vacuum carbonization. Similar observations were also recorded by other researchers in recent studies (Kumar et al., 2011; Singh et al., 2012; Wang et al., 2012). The surface areas of BCPS and BCSM are 30.84 and 67.88 m^2/g, respectively.

Table 2. BET surface areas and porosity of BCs

BC	BET surface area (m^2/g)	Micropore volume (cm^3/g)	Internal surface area (m^2/g)	Single point total volume of pores (cm^3/g)	Average pore diameter (Å)	BJH adsorption diameter (Å)	BJH desorption diameter (Å)
BCCR	126.08	0.044	40.27	0.0824	26.15	43.78	42.3
BCCS	443.96	0.1184	103.3	0.27302	24.6	45.85	43.48
BCPR	15.43	0.0167	7.074	0.0202	52.45	94.33	150.38
BCPS	30.84	0.0336	20.39	0.0377	48.87	65.98	75.56
BCSM	67.88	0.0423	47.73	0.0846	49.88	52.4	50.99

* Barret-Joyner-Halenda (BJH)

Literature tells us that microporous have pore diameters less than 20 Å and most of the adsorption takes place as a result of the closeness of graphite like walls. However, mesopores and macrospores have higher diameters 20-500 Å and greater than 500 Å, respectively. Comparing micropore volumes of the BCs as presented in Table 3 (BET and BJH). BCPR had a relatively smaller micropore volume, which indeed resulted in a lower surface area, whereas the micropore volumes of other BCs were significantly higher with BCCS recording the highest followed by BCSM, BCCR and BCPS. Interestingly, the mesopores as well as the macropore volume of BCPS was almost the same as its micropore volume, whereas micropore volumes of other BCs were significantly higher than their mesopore and macropore volumes. The pore volume distribution plots for BCs represents the amount of pores in the mesoporous range with an average pore diameter of BCCR, BCCS, BCPR, BCPS and BCSM are 26.15, 24.60, 52.45, 48.87, and 49.88 Å, respectively. The average pore diameter indicated a mesoporous structure where the presence of mesopore is important in order to enhance the adsorption capacity of BCs. These present results is in agreement with the findings of Yao et al. (2012) who concluded that lignocellulosic composition of the biomass is related to the porosity of the BC.

In recent studies of BCs, ESA ranges between 10 and 200 m^2/g of solid and the discussed BCs are in the same range. The present results indicate that without any activation process meso-macropore could be developed with the experimental process conditions. The average pore diameters determined, are in the range from mesopore diameters, indicating the BCs potential in liquid-solid adsorptions such as wastewater treatment. The charge density of BC is calculated by dividing its CEC value with the determined surface area. The charge densities of the BCs are in the following order; BCPR (0.022091 mmol/m^2) > BCPS (0.019286 mmol/m^2) > BCSM (0.010581 mmol/m^2) > BCCR (0.003828 mmol/m^2) > BCCS (0.001741 mmol/m^2). Surface charge is mainly

caused by negatively charged functional groups, therefore due to high charge density and CEC, nutrient retention by the BCs enhances.

3.6 Boehm titration

The calculated results of surface acidity were 5.25, 2.25, 3.75, 8.85 and 3.15 mmol/g for BCPS, BCPR, BCCR, BCCS and BCSM while the surface alkalinity were 2.25, 2.40, 2.40, 2.70 and 2.55 respectively after the Boehm titration. The acidic surface functionalities are instigated by the availability of carbonyl groups, lactones and phenols. Boehm titration can subsequently conduct with differences solutions to determine different functional groups. It is generally assumed that $NaHCO_3$ neutralizes only carboxylic groups, Na_2CO_3 neutralizes carboxylic and lactonic groups and NaOH neutralizes carboxylic, phenolic and lactonic groups. Therefore, the surface acidity determined by titration with NaOH will be termed as “Complete acidity”. On the other hand, surface alkalinity is more complicated topic since the cause of surface alkalinity is still controversial. However, it is assumed that the Chromenes and pyrone type groups cause the surface alkalinity. Therefore, it is accepted that titration with HCl neutralizes the available basic functionalities including ketones, as well as carbonates and other alkalinity causing species due to the presence of some ash on the BC surface (Singh et al., 2010).

There were less alkaline functional groups than acidic functional groups on the surface of BCPS and BCCR. However, BCPR was found to have had a different chemistry with its higher amount of alkaline functionalities on the surface. The maximum surface acidity was found in BCCS and BCPS (8.85 and 5.25 mmol/g), respectively, whereas BCPR had the lowest. Regarding surface alkalinity, the highest number of basic functional was again found on BCCS and BCSM (2.7 and 2.55 mmol/g), respectively whiles BCPS had the lowest. The presence of acidic surface functionalities makes BC more acidic and hydrophilic, whereas basic surface functional groups make BC more basic and hydrophobic. Therefore, it could be said that BCCS was more hydrophilic than other BCs and expected to be more acidic than the rest of the BCs. The surface acidity results of BCs in this study were relatively higher than the values reported for BCs in the literature which might be due to difference in biomasses and pyrolytic conditions.

3.7 Fourier transforms infra-red spectroscopy (FTIR)

The FTIR spectra of BCs in the IR region (wave number: 4000 – 400 cm^{-1}). Typical FTIR spectra of BCs are represented in Fig. 3. As can be observed, the FTIR of each BC was different from other regarding the intensity and availability of some specific functionality.

The spectrum of BCs was different from other regarding the intensity. The spectra of BC was characterised by the organic functional group showing a broad bands in the 3500-3400 cm^{-1} region were due to R-OH stretching or polymeric alcohol, phenol, and carboxylic acid groups. This peak was found to be prominent in all BCs. Corresponding weak R-OH band was also found in the band 3900-3700 cm^{-1} representing a monomeric alcohol, phenol and carboxylic groups. This band was not found in BCPR and BCCR. Asymmetric (CH_2, 2900 cm^{-1}) and symmetric (CH_3, 2800 cm^{-1}) C-H stretching bands were related to

aliphatic alkane functional groups. These peaks were absent in BCCR indicating the non-aliphatic nature of the BC. Relating to other BCs investigated higher intensity C-H stretching bands for the BCPR and BCSM confirmed a more aliphatic nature.

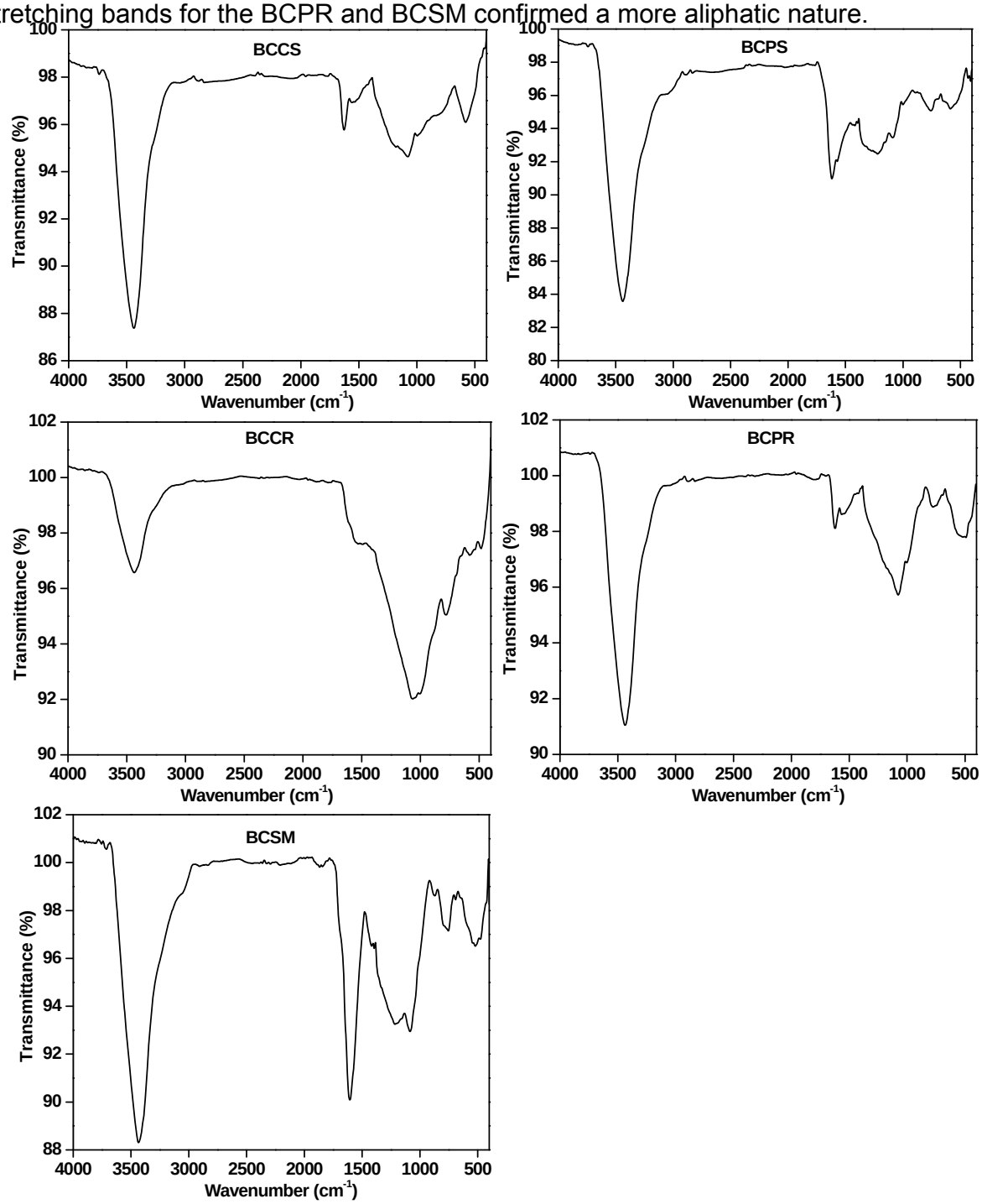

Fig.3 FTIR spectra for BCs

The –C=O stretching for carbonyls which comprises of carboxyl aldehyde, ketone, ester and acid chloride were identified in the band width 1800-1700 cm^{-1}. This band was only available in BCPR and BCSM, whiles other BCs did not show this band. It can also be seen that the above-mentioned peaks were very weak for BCPR compared to BCSM which was in agreement with its lower surface acidity. In addition to these band presence, -C=O stretching vibrations for primary and secondary amides were seen at 1630-1520 cm^{-1}. Absorption band of amide in this region probably results from carbonyl stretching vibration in the peptide bond that might be present, rather than N-H bending and C=N stretching that appear at lower wave number or intensity (Cantrell et al., 2012).

Cantrell et al.(2012) indicated that FTIR analysis of manures based BC, amides are often described as the protein-specific band, rather than the N-H bending and C-H stretching that sometimes appear at lower wave numbers. Considering BCSM, because of its higher nitrogen content, bands attributed to C=N stretching vibrations overlap with C=C absorption intensity resulting with a stronger and broad peak at 1606 cm^{-1}.

With increasing functional groups found on biochar, these were peaks at 1440 and 1390 cm^{-1} for BCPS and BBSM suggesting formation of C-H bending vibration in alkyl groups. Symmetrical bending vibration (δs CH_3) occurs near 1394.8 cm^{-1} while asymmetrical bending vibration (δ_{as} CH_3) near 1419.3 cm^{-1}. These bands are mostly found in diethyl ketones and some notable acid chlorides.

The presence of –O-C-O- stretching vibration (1300-1000 cm^{-1}) showed two small bands at 1220-1065 cm^{-1}. These bands could be attributed to symmetrical and asymmetrical aryl alkyl ethers. Emergences of these peaks were as a result of changes in vibration. These changes were attributed to the transformation products of cellulose and lignin components of the biomass feedstock. Present results were similar to finding made by Apaydin-Varol and Pütün (2012) and Tsai et al. (2012), different biomass samples and swine manure based BC, respectively. As seen in the various FTIR analyses, the presence of oxygen-based organic compounds on the surface of biochars adds significant cations exchange capacity to the soil when applied.

Aromatic C-H ring stretching were observed between 999.7-780.8 cm^{-1} for BCPS, BCCR and BCSM but were absent in BCPR and BCCS. These peaks also are attributed to aromatic C-H. Aromatic C-H peaks are indication of benzene like rings. However, Kumar et al. (2011) observed the similar peak (893 cm^{-1}) on biochar derived from switch grass and attributed it to aromatic stretching of C-H group in β-aromers or β-linked glucose polymers which were the main causes of surface alkalinity in the case of BCSM and BCCR. Similarly, Cantrell et al. (2012) also observed a similar peak (781 cm^{-1}) on swine manure-based was attributed to pyridines. BCSM showed a peak at 753.8 cm^{-1} which can be attributed to the presence of pyridine group of heterocyclic nitrogen compounds.

The FTIR spectra of the BCs displayed in Fig. 3 revealed the complex functional groups consisting of mixture of mineral and organic matter. As can be observed for the spectra, the bands below 775 cm^{-1} are probably due to C-X stretching vibrations in both organic halogens compounds (X-halogens). Bending vibration of C-Cl (775-690.6 cm^{-1}) were detected in all but BCCS and BCCR. Similar, bending vibration of aliphatic alkyl halide C-Br (528-595 cm^{-1}) was found in all but BCPR.

Stretching vibrations assigned to S-S linkage occur in the region of 500-400 cm^{-1}. This disulphide stretching vibration is very weak. The weakness of absorption and variability of this position make it have little value is structural determination (Silverstein et al., 2005). BCs FTIR peak between 490.6 and 432.9 cm^{-1} corresponds to disulphide S-S stretching vibrations. BCPR, BCPS and BCCR showed with this range.

Carrier et al. (2012) studied the surface chemistry of sugarcane bagasse produced from vacuum pyrolysis at different final process temperature ranging from 200-800 ^{o}C via FTIR analysis. Comparing the surface chemistry of the BC produced at this pyrolytic temperature, it was clear that the BC produced at this pyrolytic temperature, it was clear that the BC had similar surface functional groups, compared to this present study however, some of the peaks such as those at 3400, 2926 and 2870 cm^{-1} disappeared. These peaks correspond to stretching in hydroxyl groups and stretching in alkyl groups. The non-appearance of these peaks observed, however a new peaks around 1598 cm^{-1} C=C stretching, appeared on the BC surface. This confirms an increase in aromaticity during any types of pyrolysis as can be observed from BCCR, BCCS, BCPR, BCPS and BCSM. Similar results were made by Rambabu et al. (2013) for the FTIR analysis of fluid petroleum coke based BC activated with varying chemicals. The peaks at 3637 and 3024 cm^{-1} are attributed R-OH stretching in alcohols and C-H stretching in alkanes respectively, but new peaks from 700 to 900 cm^{-1} are attributed to an adjacent aromatic C-H stretching appeared on the BC surface. Conclusively, pyrolytic temperatures and biomass feedstock have been an important effect on the aromatic nature of the BC due to the decomposition of unsaturated chemicals structure during pyrolysis (Maroušek, 2013).

As stated earlier, the surface chemistry of the BCs are related to the biomass feedstock. The chemical composition of the biomass feedstock influences the surface functionalities. Rambabu et al. (2013) noted that during the pyrolysis or carbonization process, hemicelluloses begin to decomposition around (200-260 ^{o}C), followed by cellulose (240-351 ^{o}C) and finally lignin (280-489 ^{o}C). Kumar et al. (2011) studied the thermal degradation of switchgrass and the FTIR analyses of the BCs prepared. They again concluded that signals around 893 cm^{-1} is a characteristics of β-anomers or β-linked glucose polymers, whiles signals around 1700 cm^{-1} can be as a results of lignin and hemicelluloses.

3.8 Cationic exchange capacity (CEC)

The values of CEC for BCCR, BCCS, BCPR, BCPS and BCSM were tested as 48.26, 77.3, 34.09, 59.48 and 71.83 cmol/kg. BCCS showed the highest cationic exchange value (77.30 cmolc/kg), whereas BCPR recorded the lowest (34.09 cmolc/kg). CEC value of BCCS is similar to CEC of common soil mineral montmorillonite (75-150 cmolc/kg), When comparing the CEC values of the biochars to Kaolinite (2-15 cmolc/kg), it was seen that the value of BCCR is three times, BCCS is five times, BCPR is two times, BCPS is four times and BCSM is also five times as high as Kaolinite. The CEC of soil organic matter or humic substances range between 150-200 cmolc/kg which is much higher than the CEC values of the biochars produced. The O/C values are presented as an indicative of the presence of considerable hydroxyl, carbonyl, carboxylate, and phenolic groups which

could contribute to a higher CEC value (Lee et al., 2010). This conclusion suggests that higher CEC values could be attained of the pyrolytic/carbonization conditions are optimized for various biomasses used.

As CEC is related with the presence of acidic functional groups, the CEC of all the produced biochars were compared to the surface acidity values. As expected, BCCS which had the highest surface acidity, showed the highest CEC, while BCPR recorded the lowest CEC with a corresponding low surface acidity. Therefore, it would be expected that CEC values would decrease with increase in the pyrolytic temperature because higher pyrolysis temperature result in loss of acidic surface functional groups. All in all, it could be deduced that the biomass feedstocks as well as the pyrolytic conditions have contributed to higher acidic functionalities due to lesser or no secondary reactions.

4. CONCLUSIONS

SEM analysis indicated that BCs in this present study had a distinguishable pore size which also contributed to their high surface areas. Sharp crystalline peaks found at 2θ at d=3.35 Å and d=3.16-3.00 Å were indications of the presence of quartz (SiO_2) and calcite ($CaCO_3$), respectively, whiles these beaks were missing in BCCS. Proximate analysis indicated that BCs recorded the highest moisture content in BCCR (9.65%) whiles BCSM also recorded the highest ash content (15.22%). Consequently, the elemental analysis showed that carbon content of BCs increased from 58.97-81.28%. Atomic ratios, polarity index and aromatic ratios in these BCs were also determined. The BET surface area, micropore volume, internal surface area, single point total volume of pores, average pore diameter, BHJ adsorption and desorption diameters (Å) were also determined. The BET surface areas of BCCR, BCCS, BCPR, BCPS and BCSM were 126.08, 443.96, 15.43, 30.84 and 67.88 m^2/g, respectively. Boehm titration analysis showed that the highest surface acidity was observed for BCCS (8.85 mmol/g), lowest surface acidity was observed for BCPR (2.25 mmol/g), highest surface alkalinity was observed for BBCS (2.7 mmol/g), whereas lowest surface alkalinity was also observed for BCPS (2.25 mmol/g). The FTIR fingerprint appears to be quite different for BCs derived from different biomass feedstock. Common bands around 3600 cm^{-1} was assigned mainly to the polymeric R-OH and 1078 cm^{-1} was assigned to carbonyl esters C=O. Finally, the cation exchange capacities (CEC) of biochars were 48.26, 77.30, 34.09, 59.48 and and 71.83 cmol/kg for BCCR, BCCS, BCPR, BCPS and BCSM.

ACKNOWLEDGEMENTS

This paper was financially supported by the National Natural Science Foundation of China (21167007), the Specialized Research Fund for the Doctoral Program of Higher Education of China (20136204110003) and the Youth Science Foundation of Lanzhou Jiaotong University (2013015).

REFERENCES

Agirre, I., Griessacher, T. and Antrekowitsch, J. (2013). "Production of charcoal as an alternative reducing agent from agricultural residues using a semi-continuous semi-pilot scale pyrolysisscrew reactor", *Fuel Process. Technol.*, **106**, 114-121.

Ahmad, M., Lee, S. S., Dou, X., Sung, J., Yang, E. J. and Ok, S. Y. (2012). "Effects of pyrolysis temperature on soybean Stover and peanut shell-derived BC properties and TCE adsorption in water", *Bioresour. Technol.*, **118**, 536-544.

Angin, D. (2013). "Effect of pyrolysis temperature and heating rate on BC obtained from pyrolysis of safflower seed press cake", *Bioresour. Technol.*, **128**, 593-597.

Apaydın-Varol, E. and Pütün, A. E. (2012). "Preparation and characterization of pyrolytic chars from different biomass samples", *J. Anal. Appl. Pyrol.*, **98**, 29-36.

Cao, X. D., Ma, L. N., Gao, B. and Harris, W. (2009). "Dairy-manyure derived biochar effectively sorbs lead and atrazine", *Environ. Sci. Technol.*, **43**, 3285-3291.

Carrier, M., Hardie A. G., Ümit, U., Görgens, J. and Knoetze, J. H. (2012). "Production of char from vacuum pyrolysis of South-Africa sugarcane bagasse and its characterization as activated carbon and BC", *J. Anal. Appl. Pyrol.*, **96**, 24-32.

Chen, B. L., Zhou, D. D. and Zhu, L. Z. (2008). "Transitional adsorption and partition of non- polar and polar aromatic contaminants by BCs of pine needles with different pyrolytic temperatures", *Environ. Sci. Technol.*, **42**, 5137-5143.

Chen, X., Chen, G., Chen, L., Chen, Y., Lehmann, J. and McBride, B. M. (2011). "Adsorption of copper and zinc BCs produced form pyrolysis of hardwood and corn straw in aqueous solution", *Bioresour. Technol.*, **102**, 8877-8884.

Fraser, B. (2010). "High-tech charcoal fights climate change", *Environ. Sci. Technol.*, **44**, 548-549.

Gao, Y., Yue, Q., Gao, B., Sun, Y., Wang, W., Li, Q. and Wang, Y. (2013). "Preparation of high surface area- activated carbon from lignin of papermaking black liquor by KOH activation for Ni(II) adsorption", *Chem. Eng. J.*, **217**, 345-353.

Keiluweit, M., Nico, P. S., Johnson, M. G. and Kleber, M. (2010). "Dynamic molecular structure of plant biomass-derived black carbon (biochar)", *Environ. Sci. Technol.*, **44**, 1247-1253.

Kumar, S., Loganathan, A, V., Gupta, B, R. and Barnett, O, M. (2011). "An assessment of U(VI) removal from groundwater using BC produced from hydrothermal carbonization", *J. Environ. Manage.*, **92**, 2504-2512.

Lee, W. J., Kidder, M., Evans, R. B., Paik, S., Buchana, A. C., Garten, T. C. and Brown, C. R. (2010). "Characterization of BC produced from cornstovers for soil amendment", *Environ. Sci. Technol.*, **44**, 7970-7974.

Lehmann, J. (2007). "A handful of carbon", *Nature*, **447**: 143-144.

Lehmann, J. and Joseph, S. (2009). "*Biochar for Environmental Management: Science and Technology*", Earthscan. Sterling, USA.

Liang, B., Lehmann, L., Sohi, S. P., Thies, J. E., O´Neil, B., Trujilo, L., Gaunt, J., Solomon, D., Grossman., J., Neves, E., and Luizao, F. J. (2010). "Black carbon affects the cycling on non-black carbon in soil", *Org. Geochem*., **41**, 206-213.

Liu, Z. and Zhang, F. S. (2009). "Removal of lead from water using biochars prepared from hydrothermal liquefaction of biomass", *J. Hazard. Mater.*, **167**, 933-939.

Maroušek, J. (2013). "Removal of hardly fermentable ballast from the maize silage to accelerate biogas production", *Ind. Crop. Prod.*, **44**, 253-257.

Marris, E. (2006) "Putting the carbon back: Black is the new green", *Nature*, **442**: 624-626.

Mohammed, F. M., Roberts, E. P., Hill, A., Campen, A. K. and Brown, N. W. (2011). "Continuous water treatment by adsorption and electrochemical regeneration", *Water Res.*, **45**, 3065-3074.

Nan, Z. R. and Li, J. J. (2000). "Study on the distribution and behavior of selected metals (Cd, Ni, Pb) in cultivated soil profile in arid zone (take Baiyin region as an example)", *Arid Zone Res.*, **17**, 39-45.

Rambabu, N., Azargohar, R. and Adjaye, J. (2013). "Evaluation and comparison of enrichment effieiciency of physical/chemical activations and functionalized activated carbons derived from fluid petroleum coke for environmental applications", *Fuel Process. Technol.*, **106**, 501-510.

Regmi, P., Moscoso, J. L. G., Kumar, S., Cao, X., Mao, J. and Schafran, G. (2012). "Removal of copper and cadmium from aqueous solution using switchgrass biochar produced via hydrothermal carbonization process", *J. Environ. Manage.*, **109**, 61-69.

Renner, R. (2007). "Rethinking biochar", *Environ. Sci. Technol.*, **41**, 5932-5933.

Roberts, K. G., Gloy, B. A., Joseph, S., Scott, N. R. and Lehmann, J. (2010). "Life cycle assessment of biochar systems: estimating the energetic, economic, and climate change potential", *Environ. Sci. Technol.*, **44**, 827-833.

Silverstein, M. R., Webster, X. F. and Kiemle, J. D. (2005). "*Spectrometric identification of organic compounds*", 7th Edition, John Wiley & Sons, USA.

Singh, B., Singn, B. P. and Cowie, A. L. (2010). "Characterization and evaluation of BCs for their application as a soil amendment', *Aust. J. Soil Res.*, **48**, 516-525.

Singh, S., Nahil, A. M., Sun, X., Wu, C., Chen, J., Shen, B. and Williams, T. P. (2012). "Novel application of cotton stalk as a waste derived catalyst in the low temperature SCR-deNOx process", *Fuel*, **105**, 585-594.

Tong, X., Li, J., Yuan, J. and Xu, R. (2011). "Adsorption of Cu (II) by biochars generated from three crop straws", *Chem. Eng. J.*, **172**, 828-834

Tsai, W. T., Liu, S. C., Chen, R. H., Chang, M. Y. and Tsai, L. Y. (2012). "Textural and chemical properties of swine-manure derived BC pertinent to its potential use as a soil amendment", *Chemosphere*, **89**, 198-203.

Wang, T., Cheng, J., Liu, J., Zhang, C. and Yu, X. (2012). "Effect of BC amendment on bioavailability of pesticide chlorantraniliprole in soil to earthworm", *Ecotoxic. Environ. Safety*, **83**, 96-101.

Yao, Y., Gao, B., Chen, H., Jiang, L., Inyang, M., Zimmerman, R. A., Cao, X., Yang, L., Xue, Y. and Li, H. (2012). "Adsorption of sulfamethoxazole on BC and its impact on reclaimed water irrigation", J. Hazard. Mater., **209-210**, 408-413.

Zhang, M., Gao, B., Varnoosfaderani, S., Hebarb, A., Yao, Y. and Inyang, M. (2013). "Preparation and characterization of a novel magnetic BC for arsenic removal", *Bioresour. Technol.*, **130**, 457-462.

Zhou, S., Mourant, D., Lievens, C., Wang, Y., Li, C. Z. and Garcia-Perez, M. (2013). "Effect of sulphuric acid concentration on yield and properties of bio-oils obtained from the auger and fast pyrolysis of Douglas Fir", *Fuel*, **104**, 536-546.

Zimmerman, A. R. (2010). "Abiotic and microbial oxidation of laboratory-produced black carbon (biochar)", *Environ. Sci. Technol.*, **44**, 1295-1301.